SUPPLEMENTARY INFORMATION for Manuscript

Local Spin Dynamics of Iron Oxide Magnetic Nanoparticles dispersed in different solvents with variable Size and Shape : a ^{1}H NMR Study

M. Basini[a], T.Orlando[c] P. Arosio[a], M. F. Casula[b], D. Espa[b], S. Murgia[b], , C. Sangregorio[d,e], C.Innocenti[d,e] and A. Lascialfari[a, f].

[a]*Dipartimento di Fisica and INSTM,Università degli Studi di Milano, Milano, Italy,*

[b]*Dipartimento di Scienze Chimiche e Geologiche and INSTM, Università di Cagliari, Monserrato, Italy*

[c]*EPR Research Group, Max Planck Institute for Biophysical Chemistry, Göttingen, Germany*

[d] *Dipartimento di Chimica and INSTM, Università degli studi di Firenze, Sesto F.no , Italy*

[e]*ICCOM-CNR, Sesto F.no, Italy*

[f]*Istituto di Nano scienze, CNR-S3, Modena, Italy.*

Water-based dispersions. Sample S8_Hex, which was made out of nearly spherical nanocrystals with average diameter 8.5 nm, was transferred into a water-based dispersant solution (water content > 96 wt%) containing monoolein and lauroylcholin, producing sample S8_Wat. DLS shows that a significant average diameter increase is observed going from sample S8_Hex to sample S8_Wat. In agreement, bright field TEM images (Figure S1) show that the MO/LCh/W system is able to stabilize the MNPs in water as singular entities or as aggregates. The magnetic nanoparticles appear as well-separated, confirming that the original capping agent (oleic acid) is retained on the nanocrystal surface. It is proposed that both monoolein and lauroylcholin are present on the surface of the nanocrystals, either as intercalated or interdigitated into oleic acid alkyl chains. Systematic investigation of the structure of the suspension of nanoparticles in the MO/LCh/W dispersant system is currently underway. [SI_1]

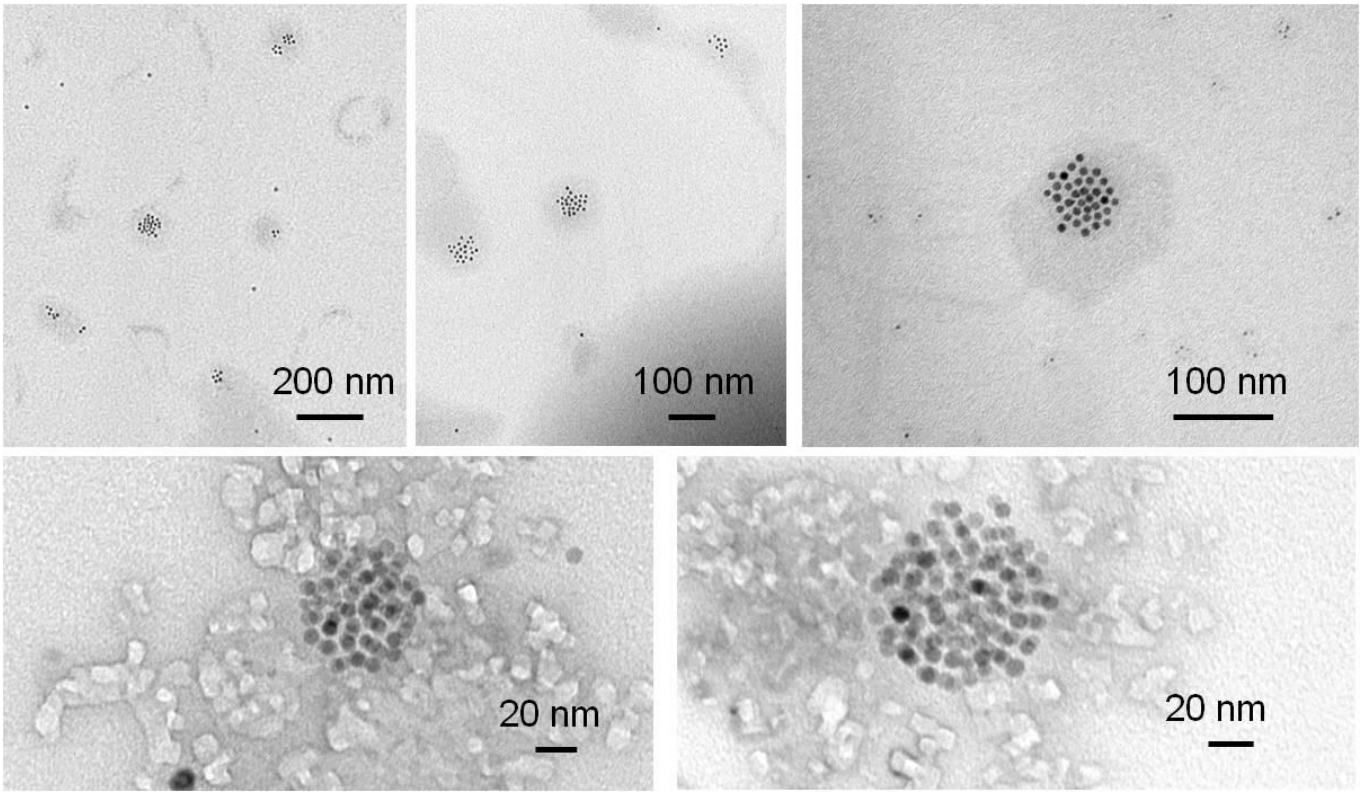

Fig S_1 TEM images of the S8_Wat sample showing the iron oxide nanocrystals dispersed in a water-based MO/LCh/W system.

XRD characterization. X-Ray diffraction patterns were collected using Cu Kα radiation and are reported in Figure S_1 and phase analysis was performed by comparison with the Powder Diffraction Files database.[SI_2 All the samples show the occurrence of very broad diffraction peaks whose position and relative intensity can be ascribed to the presence of a spinel ferrite iron oxide nanocrystalline phase. Due to the very similar lattice parameters and due to peak broadening, diffraction techniques do enable to discriminate unambiguously among the two magnetic spinel iron oxide phases, maghemite γ-Fe_2O_3 and magnetite Fe_3O_4, which is usually performed through spectroscopy techniques. [SI_3] Samples S8_Hex/Wat and sample S17_Hex also show a shoulder at $2\theta \approx 36.5$ which accompanies the main reflection of the spinel phase at $2\theta \approx 35.5$ and which can be ascribed to the occurrence of wustite phase, previously found in iron oxide colloidal nanocrystals prepared by oleate precursors. [SI_4] The diffraction profile exhibits a sharpening going from sample S3_Hex to sample S17_Hex, suggesting an increase in the average nanocrystal size, as demonstrated by TEM data.

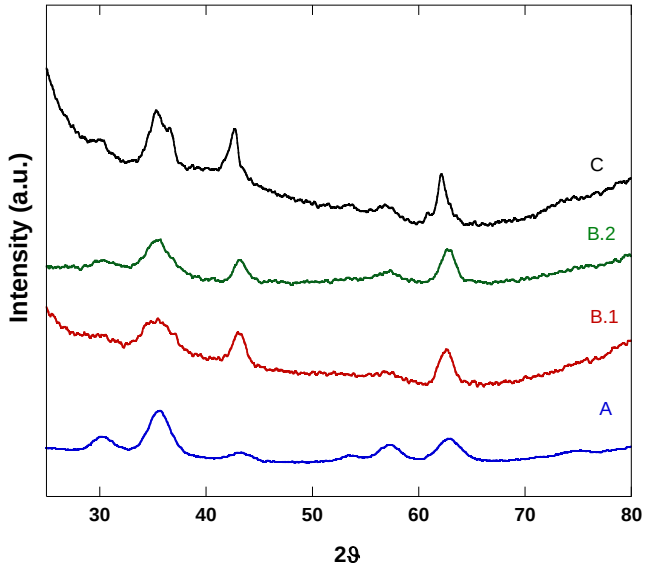

Fig. S_2 X-ray diffraction pattern obtained using Cu Kα radiation: from bottom to top samples **S3_Hex (A)**, **S8_Hex (B.1)**, **C8_Hex (B.2)**, **S17_Hex (C)**.

S3_Hex H (Oe)	**μ**	**σ^2**	**E_b ZFC** (K)	**δE_b ZFC** (K)	**τ_0** (rad/s)	**T_0** (K)	**τ_N AC** (rad/s)
50	3.49	0.56	43.3	37.8	5.5×10^{-8}	4.2	4.7×10^{-8}
200	2.35	1.43	21.4	38.2	1.5×10^{-6}	5.2	1.7×10^{-6}
300	2.46	0.54	15.3	13.0	5.4×10^{-6}	5.7	1.7×10^{-6}

S8_Hex H (Oe)	**μ**	**σ^2**	**E_b ZFC** (K)	**δE_b ZFC** (K)	**τ_0** (rad/s)	**T_0** (K)	**τ_N AC** (rad/s)
50	5.67	0.29	334	194	2.4×10^{-11}	30.5	7.0×10^{-10}
100	5.59	0.36	320	210	4.78×10^{-11}	30.4	3.1×10^{-10}
200	5.65	0.37	343	231	2.5×10^{-11}	29.7	8.1×10^{-11}
500	4.30	1.53	158	301	1.7×10^{-8}	35.4	2.1×10^{-8}
700	2.63	3.03	63	279	1.4×10^{-6}	39.7	1.8×10^{-6}

C8_Hex **H (Oe)**	**μ**	**σ^2**	**E_b ZFC** (K)	**δE_b ZFC** (K)	**τ_0** (rad/s)	**T_0** (K)	**τ_N AC** (rad/s)
50	4.64	0.68	146.3	145	1.5×10^{-9}	18.2	8.8×10^{-10}
100	4.85	0.61	174	160	3.7×10^{-10}	17.3	9.6×10^{-10}
200	4.43	1.04	142	193	1.8×10^{-9}	18.3	3.0×10^{-9}

S17_Hex **H (Oe)**	**μ**	**σ^2**	**E_b ZFC** (K)	**δE_b ZFC** (K)	**τ_0** (rad/s)	**T_0** (K)	**τ_N AC** (rad/s)
50	7.35	0.17	1683.5	711.2	4.4×10^{-14}	160	7.3×10^{-9}
100	6.94	0.47	1304	1007	8.9×10^{-13}	170	2.1×10^{-8}
200	5.97	1.32	756	1249.5	1.7×10^{-10}	183.5	1.1×10^{-9}
350	3.98	3.17	260	1242	-	-	-

Tab. S_1 List of the main magnetic parameter as a function of field. From left: T_B is the spin blocking temperature; μ and σ^2 are the mean and variance lognormal distribution calculated from the energy barrier distribution E_B and δE_B; τ_0 and T_0 are the attempt time and the interaction energy calculated from the fit of AC experimental data with the Vouguel-Fulcher equation; τ_N is the Neèl time (magnetization reversal time).

Sample	M_V x 10^5 (A/m)	$\Delta\omega$ x 10^6 (rad/s)	τ_D x 10^{-9} (s)	$\Delta\omega\tau_D$	$r_2^{(60\ MHz)}$ ($s^{-1}mM^{-1}$)	$\varphi_{intra} r_2 / M^2_v$ ($s^{-1}mM^{-1}m^2A^{-2}$)
S3_Hex	1.28	2.2	18.17	0.040	25	1.52 E-9
S8_Hex	2.3	4.1	6.97	0.028	17	3.2 E-10
C8_Hex	2.1	3.7	6.34	0.023	26	5.9 E-10
S17_Hex	1.6	2.9	17.97	0.052	46	1.8 E-9

Tab.S_2 Lists of parameter used to test Vuong model nanoparticle in the MAR regime (refer to fig.8 in the paper text)

References

[SI_1] M. F. Casula et al, in preparation

[SI_2] PDF-2 File, ICDD International Centre for Diffraction Data, 1601 Park Lane, Swarthmore, USA,

[SI_3] A. Corrias, G. Mountjoy, D. Loche, V. Puntes, A. Falqui, M. Zanella, W. J. Parak, M.F. Casula, *Identifying spinel phases in nearly monodisperse iron oxide colloidal nanocrystals***,** J. Phys. Chem. C, **113**, 18667, (2009)

[SI_4] M.F. Casula, Y-w Jun, D. J. Zaziski, E.M. Chan, A. Corrias, A. P. Alivisatos *The concept of Delayed Nucleation in nanocrystal growth demonstrated for the case of Iron Oxide Nanodisks*, J. Am. Chem. Soc., **128**, 1675 (2006)